

Real-Time CRLB based Antenna Selection in Planar Antenna Arrays

Masoud Arash, *Student member, IEEE*, Ivan Stupia, *Member, IEEE*, Luc Vandendorpe, *Fellow, IEEE*

Abstract

Estimation of User Terminals' (UTs') Angle of Arrival (AoA) plays a significant role in the next generation of wireless systems. Due to high demands, energy efficiency concerns, and scarcity of available resources, it is pivotal how these resources are used. Installed antennas and their corresponding hardware at the Base Station (BS) are of these resources. In this paper, we address the problem of antenna selection to minimize Cramer-Rao Lower Bound (CRLB) of a planar antenna array when fewer antennas than total available antennas have to be used for a UT. First, the optimal antenna selection strategy to minimize the expected CRLB in a planar antenna array is proposed. Then, using this strategy as a preliminary step, we present a two-step antenna selection method whose goal is to minimize the instantaneous CRLB. Minimizing instantaneous CRLB through antenna selection is a combinatorial optimization problem for which we utilize a greedy algorithm. The optimal start point of the greedy algorithm is presented alongside some methods to reduce the computational complexity of the selection procedure. Numerical results confirm the accuracy of the proposed solutions and highlight the benefits of using antenna selection in the localization phase in a wireless system.

Index Terms

Antenna Selection, CRLB, Angle of Arrival.

I. INTRODUCTION

Localization of UTs is an indispensable part of wireless systems. On the one hand, many applications, like auto-driving cars and health services, directly require continuous tracking of

The authors are with the Institute of Information and Communication Technologies, Electronics and Applied Mathematics (ICTEAM), Université Catholique de Louvain, 1348 Louvain-la-Neuve, Belgium (E-mail: masoud.arash@uclouvain.be).

This work has been submitted to the IEEE for possible publication. Copyright may be transferred without notice, after which this version may no longer be accessible.

UT's locations. On the other hand, using location information, higher data rates with higher efficiencies can be transferred to the UTs [1]. In all of these applications, Angle of Arrival (AoA) information plays a key role.

A general criterion to evaluate the capability of a system to localize UTs is CRLB. Numerous works have studied the CRLB in different system models [2], [3]. Many parameters of a system affect the CRLB. In particular, the arrangement of antennas at the receiver side has substantial influence over the ability of AoA estimation. A linear [4], concentric [5], or planar [6] antenna array each has certain pros and cons. Planar antenna array provides wide aperture and uses assigned space for antenna array more efficiently (making them a suitable choice for Massive MIMO systems) [7]. Also, studies for planar antenna arrays can be easily generalized to newly emerging concept of large intelligent surfaces [8], [9].

Antenna selection is a solution for various challenges in multi-antenna systems. The number of active antennas may be limited by energy efficiency concerns [10], hardware shortage or complexity [11], or multi-casting services where different antennas provide different services to different UTs [12]. Another motivation for antenna selection is when using all of the available antennas may surpass the required accuracy of the system [13]. When the number of antennas needed to establish a wireless link is fewer than the total available antennas, selecting a specific set of antennas allows certain aspects of the system's performance to be significantly improved, e.g., the ability to estimate AoA with higher accuracy.

In this regard, [14] proposes a neural network selection method that aims to minimize the log-determinant of CRLB in a radar system. In [15] authors present a greedy algorithm for sensor selection in distributed radars where the objective function to minimize is the probability of error. Another use of greedy algorithms to select antennas is studied in [13] where the goal is to minimize minimum square error in a distributed system, using a knapsack problem formulation. In [16] authors introduced an antenna selection strategy that uses a cyclic algorithm to minimize posterior CRLB in a 2D scenario for a compact MIMO radar. In [17] authors used a Dinkelbach like algorithm to minimize CRLB of AoA when desired parameters for estimation were AoA and azimuth of a UT. An unsupervised learning approach is used to minimize total CRLB for azimuth and AoA of a UT in [18].

The main point in minimizing CRLB for AoA in 3D scenario is that as it is a combined function of both antenna set and AoA, without knowledge of AoA, it will not be possible to minimize CRLB, and if AoA is known, there will be no need to minimize it. In this regard, in

[3] we presented a greedy antenna selection approach that aims to minimize the expected CRLB of AoA in a 3D scenario. With the help of the expectation (over all possible values of AoA), it is possible to remove the effects of the instantaneous AoA and minimize it.

Moreover, a major difference of employing a greedy algorithm in a compact planar antenna array with the distributed case, like the ones considered in [15], [13], is that in the case of a compact array, the first three antennas have to be chosen together. This is because at least three antennas are required to create a plane, so the CRLB formulation of a planar antenna array can be used. Only after the selection of these three antennas, the greedy approach by selecting one antenna at each step can be implemented.

A key feature of greedy algorithm is its simplicity, which makes it possible to run it quickly. Although the procedure of greedy algorithm is trivial, if its starting set (that is composed of three antennas) is selected properly, the greedy algorithm is able to obtain a performance quite close to the global optimum. The start set is especially important when few antennas are going to be selected because antennas in the start set make up a considerable portion of the total utilized antennas. It should be noted that an exhaustive search for this initial set usually has a substantial computational cost.

In the first part of this work, in continuation of our previous work [3], an optimal antenna selection strategy whose objective is to minimize the expected CRLB for a planar antenna array in a 3D setting is proposed, where the effects of an unknown elevation is also considered in the calculation of the CRLB. This antenna selection strategy only requires the possible range of AoA and its distribution to take the expectation from the CRLB. The advantage of this selection procedure is that the usage priority of antennas can be determined prior to implement the system.

In the next part, to address the problem of lack of knowledge about AoA, we present a double-stage antenna selection procedure that aims to minimize instantaneous CRLB of AoA. In the first step, a crude estimation of AoA is made using antennas that are selected to minimize expected CRLB. Then based on this estimation, a greedy algorithm with an optimal start point is employed to minimize the instantaneous CRLB. To reduce the computational complexity of the greedy algorithm, especially for its initial start set, we present the optimal start set for every value of AoA. Furthermore, by using the characteristics of the $CRLB_{\theta}$ we prove that in each step of the greedy algorithm, by searching only half of the available antennas, the contribution of all antennas can be evaluated. This proposition will further reduce the computational complexity of utilizing the greedy algorithm. In the end, we generalize our method to a multi-user scenario

to show that the same approach can also be beneficial when there are more than one UT.

The contribution of the paper is summarized as the following:

- The optimal antenna selection strategy to minimize the expected CRLB of AoA estimation in planar antenna arrays in a 3D scenario is presented.
- By using the antenna selection for minimizing the expected CRLB, a double-stage antenna selection method is developed that aims to minimize instantaneous CRLB of AoA with the help of a greedy algorithm whose optimal start point is presented.

Notation: Boldface lower case is used for vectors, \mathbf{x} , and upper case for matrices, \mathbf{X} . \mathbf{X}^H denotes conjugate transpose \mathbf{X} , $\mathbb{E}_x\{\cdot\}$ is expectation operator w.r.t x , $j = \sqrt{-1}$, $|\cdot|$ stands for absolute value of a given scalar variable, \otimes is Kronecker product, $diag(\mathbf{x})$ is a diagonal matrix with the elements of vector \mathbf{x} on the main diagonal, \cup is union operator and tr is trace operator. Also, \mathbf{I}_K is $K \times K$ identity matrix.

The remaining of the paper is organized as follows. In section II the system model is presented. In section III the CRLB of presented system model is calculated. Section IV presents both the antenna selection method to minimize expected CRLB and the proposed two stage antenna selection method that aims to minimize instantaneous CRLB. In section V we extend our model to the multi-user case. Finally, section VI studies the performance of the proposed methods through simulations.

II. SYSTEM MODEL

We consider the uplink of a single-cell MIMO system with a BS at the center, equipped with $(M + 1)^2$ antennas. $M + 1$ antennas are installed along each of the x and y axes. For mathematical tractability and clarity, it is assumed that M is an even number. On each axis, adjacent antennas are separated by distance d (Fig.1). There is a UT in the cell, and the BS uses pilot signals transmitted by the UT to localize the UT¹. For clarity, we assume that there is only one dominant path. However, our concept can be applied for any channel model (like the dense multi-path channel model that we used in [3], [4]), i.e., our method is independent of the channel model. The received signal at the BS is

$$\mathbf{y} = \mathbf{a}_R h_d s + \mathbf{n}, \quad (1)$$

¹Indeed, there can be more than one UT, but they have to use different frequency or time slot and the following concepts can be applied to each of them.

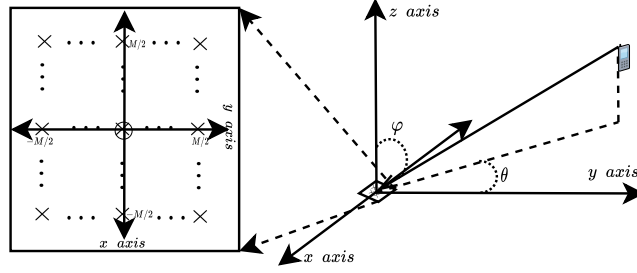


Figure 1: Antenna configuration at the BS w.r.t the UT.

where h_d is the channel coefficient for the dominant path of the UT, \mathbf{s} is the transmitted pilot by the UT and $\mathbf{n} \sim \mathcal{CN}(0, \sigma_n^2 \mathbf{I}_M)$ is additive white Gaussian noise. Also, \mathbf{a}_{Rx} is the steering vector of BS antenna array response, where θ_k and φ_k are the UT's AoA and azimuth. The m th element of \mathbf{a}_{Rx} is [6]

$$\mathbf{a}_R(\theta, \varphi)_m = e^{-j\beta \sin(\varphi_k)((m_1-1) \cos(\theta_k) + (m_2-1) \sin(\theta_k))}, \quad (2)$$

$$m = (m_2 - 1)(M + 1) + m_1, \quad m_1 = 1, \dots, M + 1, \quad m_2 = 1, \dots, M + 1,$$

where $\beta = \frac{2\pi d}{\lambda}$ and λ is the wavelength of pilots.

III. CRLB

In this part, we obtain the formulation of $CRLB_\theta$ that is the CRLB for the estimation of the θ , when $F \leq (M + 1)^2$ antennas are activated (and the rest of them are not used). As the CRLB of θ in a planar antenna array is well studied in the literature (namely in [3], [17]), we just briefly explain how the same results can match our system model with minor changes in the $CRLB$ calculations².

The vector of the desired variables is $\boldsymbol{\eta} = [\theta \ \varphi]$. Defining $\hat{\boldsymbol{\eta}}$ as the unbiased estimator of $\boldsymbol{\eta}$, its mean square error is lower bounded as

$$\mathbb{E}_{\mathbf{y}|\boldsymbol{\eta}}\{(\boldsymbol{\eta} - \hat{\boldsymbol{\eta}})(\boldsymbol{\eta} - \hat{\boldsymbol{\eta}})^T\} \geq \mathbf{CRLB} = \mathbf{J}^{-1}, \quad (3)$$

where \mathbf{J} is Fisher information matrix and can be written in block matrix form as [2]

$$\mathbf{J} = \begin{bmatrix} J_{\theta, \theta} & J_{\theta, \varphi} \\ J_{\varphi, \theta} & J_{\varphi, \varphi} \end{bmatrix}, \quad (4)$$

²For detailed calculation, please refer to [3], section III.

and

$$J_{a,b} = \mathcal{R}e\left[\left(\frac{\partial \mathbf{w}}{\partial \boldsymbol{\eta}_a}\right)^H \left(\frac{\partial \mathbf{w}}{\partial \boldsymbol{\eta}_b}\right)\right], \quad (5)$$

in which $\mathbf{w} \triangleq \mathbf{a}_{R_x} h_d s$ and $a, b \in \{\theta, \varphi\}$. Therefore, using block matrix inversion properties, $CRLB_\theta$ is

$$CRLB_\theta = \frac{\sigma_n^2}{2} (J_{\theta,\theta} - J_{\theta,\varphi} J_{\varphi,\varphi}^{-1} J_{\varphi,\theta})^{-1}. \quad (6)$$

From [3], equations (18-19), we know that

$$\begin{aligned} J_{\theta,\theta} &= \beta^2 |h_d|^2 \sin^2(\varphi) (tr(\tilde{\boldsymbol{\Sigma}}_1^2) \sin^2(\theta) + tr(\tilde{\boldsymbol{\Sigma}}_2^2) \cos^2(\theta) - 2tr(\tilde{\boldsymbol{\Sigma}}_1 \tilde{\boldsymbol{\Sigma}}_2) \cos(\theta) \sin(\theta)), \\ J_{\varphi,\varphi} &= \beta^2 |h_d|^2 \cos^2(\varphi) (tr(\tilde{\boldsymbol{\Sigma}}_1^2) \cos^2(\theta) + tr(\tilde{\boldsymbol{\Sigma}}_2^2) \sin^2(\theta) + 2tr(\tilde{\boldsymbol{\Sigma}}_1 \tilde{\boldsymbol{\Sigma}}_2) \cos(\theta) \sin(\theta)), \\ J_{\theta,\varphi} &= \beta^2 |h_d|^2 \sin(\varphi) \cos(\varphi) (tr(\tilde{\boldsymbol{\Sigma}}_2^2 - \tilde{\boldsymbol{\Sigma}}_1^2) \sin(\theta) \cos(\theta) + tr(\tilde{\boldsymbol{\Sigma}}_1 \tilde{\boldsymbol{\Sigma}}_2) (\cos^2(\theta) - \sin^2(\theta))). \end{aligned} \quad (7)$$

where $\tilde{\boldsymbol{\Sigma}}_1$ and $\tilde{\boldsymbol{\Sigma}}_2$ are $F \times F$ selected matrices from $(M+1)^2 \times (M+1)^2$ $\boldsymbol{\Sigma}_1$ and $\boldsymbol{\Sigma}_2$ matrices and

$$\begin{aligned} \boldsymbol{\Sigma}_1 &= \mathbf{I}_{M_2} \otimes \text{diag}(-M/2, \dots, M/2), \\ \boldsymbol{\Sigma}_2 &= \text{diag}(-M/2, \dots, M/2) \otimes \mathbf{I}_{M_1}. \end{aligned} \quad (8)$$

The main points of obtaining (7) from [3] are two. First, due to absence of multipath signals (caused by a different system model), the almost sure convergence in [3] is replaced with equality in (7). Second, because there is only one UT, most of matrices are converted to scalars (including the $CRLB_\theta$). By replacing (7) in (6) and after some algebraic operations, we obtain the $CRLB_\theta$ as

$$CRLB_\theta = \frac{tr(\tilde{\boldsymbol{\Sigma}}_1^2) \cos^2(\theta) + tr(\tilde{\boldsymbol{\Sigma}}_2^2) \sin^2(\theta) + 2tr(\tilde{\boldsymbol{\Sigma}}_1 \tilde{\boldsymbol{\Sigma}}_2) \cos(\theta) \sin(\theta)}{\rho_k \beta^2 |h_d|^2 (tr(\tilde{\boldsymbol{\Sigma}}_1^2) tr(\tilde{\boldsymbol{\Sigma}}_2^2) - tr(\tilde{\boldsymbol{\Sigma}}_1 \tilde{\boldsymbol{\Sigma}}_2)^2) \sin^2(\varphi)}. \quad (9)$$

By definition, $CRLB_\theta$ indicates the lowest possible error for any estimator for the considered system model. In this regard, $CRLB_\theta$ can be seen as an intrinsic characteristic to the system, as it is a function of system settings, and any unbiased estimator is bound to have a higher or equal variance as $CRLB_\theta$. This makes it a valuable parameter for various optimizations, namely antenna selection. If $CRLB_\theta$ is optimized, the performance of any estimator that will be utilized in the system will be improved. Based on this, we choose $CRLB_\theta$ as the cost function of the antenna selection optimization problem, so its outcome can be used for any estimation method.

IV. ANTENNA SELECTION

In this section, the antenna selection in the localization phase is studied, and two antenna selection methods are proposed. In the first selection method, we use the expected value of $CRLB_\theta$ as the cost function to minimize. Then, by using this method, we develop another antenna selection strategy whose cost function is instantaneous $CRLB_\theta$. We focus on the selection process and assume that number of required antennas, F , is given.

Antenna selection is one of the proposed solutions in the literature to address hardware shortage [19], or energy efficiency [10]. The general goal of antenna selection is to select a subset of antennas that results in the highest possible performance for the number of selected antennas. In [3] we have proposed a greedy antenna selection strategy that aims to minimize expected $CRLB_\theta$ for a planar antenna array, where expectation is over all possible realizations of AoA.

In [17] authors presented an antenna selection to minimize $CRLB_\theta$ for planar antenna array whose reference point is at the center of the array. The antenna set is selected based on the actual AoA using the Dinkelbach algorithm for minimization. The problem with this approach is that AoA has to be known before minimization. This means that the antenna selection cannot be used for the AoA estimation phase. Moreover, the complexity of the Dinkelbach algorithm may increase the time consumption of the antenna selection procedure. To overcome these problems, we propose a real-time antenna selection approach.

Our method is composed of two steps. The first phase is when the transmission of pilot signals by UT is not yet begun. In this phase, the only available information at the BS is the possible range and distribution of the AoA. For example, if the space division multiplexing is not used and the BS has to cover all of the cell, this range would be $[0, 2\pi)$. In this step, we turn on F_p antennas to make a crude estimation of the received AoA to have a general idea about where the UT is. The value of F_p can be defined by other criteria, like the total energy consumption of the BS. These F_p antennas are selected to minimize the expected $CRLB_\theta$ over the possible range of the AoA. In this step, we will use a certain percentage of the total transmitted pilot snapshots to acquire a preliminary estimation of the AoA (we call this estimation θ_p).

After acquiring the θ_p , we can use it to minimize the $CRLB_\theta$. By virtue of the θ_p , we can select a subset of the antennas that specifically minimize the $CRLB_\theta$ instead of its expectation. Minimizing (9) is a Combinatorial optimization problem. We use a greedy algorithm and present its optimal starting point. The greedy algorithm is chosen for the optimization due to two main

reasons. First, it can be run in real-time and very fast, thanks to its simplicity. The significance of running time is because this part of the selection process is done while BS is receiving pilot signals and extra delay in the selection process will result in missing transmitted snapshots by the UT. Second, the greedy algorithm has high level of performance. Later in the numerical result section, we show that the greedy algorithm (with the optimal starting point) obtains almost the same performance as the global search with much lower computational complexity. In the greedy approach, one antenna that reduces the $CRLB_\theta$ more than others is selected in each step.

Therefore, the steps of the antenna selection algorithm can be summarized as the following:

- 1) *Preliminary stage*: $F_p \geq 3$ antennas are selected in a way to minimize $\mathbb{E}_\theta\{CRLB_\theta\}$. BS turns on these antennas and awaits for the reception of the pilot signals from the UT. Then, it uses these antennas alongside a percentage of the total snapshots to make a Preliminary estimation of θ (that is called θ_p).
- 2) *Main stage*: Based on the θ_p , a set of antennas are selected to minimize $CRLB_\theta$ using a greedy algorithm. This set will use the remaining snapshots of the pilot signals to estimate θ .

Remark 1. *In addition to helping the antenna selection procedure, θ_p can be used to reduce the computational complexity of the estimation of θ in the Main stage. For example, in methods like ML or MUSIC where a certain range has to be searched for the estimation, only the vicinity of θ_p (with a certain margin) can be the prime candidate to be searched. This reduces the search area and reduces estimation time.*

In the following subsections, the antenna selection of each step is explained.

A. Preliminary Stage

In this stage, the only available information is the total possible range of θ . As $CRLB_\theta$ is a function of both antennas set and θ , we have to remove its dependency to θ (based on the available information) to be able to use $CRLB_\theta$ as a cost function for minimization. In order to do so, by noting that $\theta \sim U[0, 2\pi)$, the expectation of $CRLB_\theta$ over θ will be

$$\mathbb{E}_\theta\{CRLB_\theta\} = \frac{1}{2\rho_k\beta^2|h_d|^2\sin^2(\varphi)} \times \underbrace{\left(\frac{tr(\tilde{\Sigma}_{p_1}^2) + tr(\tilde{\Sigma}_{p_2}^2)}{(tr(\tilde{\Sigma}_{p_1}^2)tr(\tilde{\Sigma}_{p_2}^2) - tr(\tilde{\Sigma}_{p_1}\tilde{\Sigma}_{p_2})^2)} \right)}_{U(S)}, \quad (10)$$

where $\tilde{\Sigma}_{p_1}$ and $\tilde{\Sigma}_{p_2}$ contain the corresponding values of F_p selected antennas from Σ_1 and Σ_2 , respectively. The only part related to the antenna set in (10) is $U(\mathcal{S})$, so we have to minimize it. First, we explain the process in detail, and then we present and prove it in a theorem.

The optimal antenna selection strategy to minimize $U(\mathcal{S})$ is composed of various steps that depend on the value of the F_p . If $F_p \leq 5$, in addition to the reference point, the four antennas at the corners of the array (i.e. $S_{p_1} = \{(\frac{M}{2}, \frac{M}{2}), (-\frac{M}{2}, \frac{M}{2}), (\frac{M}{2}, -\frac{M}{2}), (-\frac{M}{2}, -\frac{M}{2})\}$) are optimal choices and all of them have the same priority to be selected. This means that if for example, $F_p = 3$, either combination of three antennas from S_{p_1} will result in the same value of $U(\mathcal{S})$. For $5 < F_p \leq 13$, the next optimal choices are neighboring antennas of the four antennas at S_{p_1} in the outer most rectangle of the array, i.e. $S_{p_2} = \{(\frac{M}{2} - 1, \frac{M}{2}), (1 - \frac{M}{2}, \frac{M}{2}), (\frac{M}{2}, \frac{M}{2} - 1), (-\frac{M}{2}, \frac{M}{2} - 1), (\frac{M}{2}, 1 - \frac{M}{2}), (-\frac{M}{2}, 1 - \frac{M}{2}), (\frac{M}{2} - 1, -\frac{M}{2}), (1 - \frac{M}{2}, -\frac{M}{2})\}$. Again, all of the antennas at S_{p_2} have the same priority to be selected, and if $5 < F_p < 13$, any combination from S_{p_2} (in addition to all of the antennas in S_{p_1}) will result in the same value for $U(\mathcal{S})$. For $13 < F_p \leq 21$, the neighbors of the ones selected for $5 < F_p \leq 13$ in the outermost rectangle of the array are optimal choices and so on. Therefore, the process is to start with the four antennas at S_{p_1} at the corners and start to select their neighbor antennas and move toward other corners. An example of this process for $M = 6$ is represented graphically at Fig. 2. In this figure, four red antennas have the highest priority to be selected. After selecting all of them, we move in both available directions (shown by solid arrows) to select antennas with blue markers. All antennas with blue markers have the same priority. Then the same procedure is continued by moving in the same directions (showed by dashed arrows) to obtain the next set of antennas, marked by green markers. When all antennas from the outermost rectangle are selected, the same process is repeated from the second outermost rectangle. The following theorem summarizes the optimal selection procedure.

Theorem 1. *The optimal antenna selection strategy to minimize $\mathbb{E}_\theta\{CRLB_\theta\}$ for $\theta \sim U[0, 2\pi)$ is to start from the four antennas at the corner of the array and then, from each corner, move toward other two corners, selecting antennas from the outermost rectangle. Antennas that have the same distance from their closest corner antenna, have the same priority for selection. When all antennas at the outermost rectangle are selected, the same procedure is repeated in the second outermost rectangle and so on.*

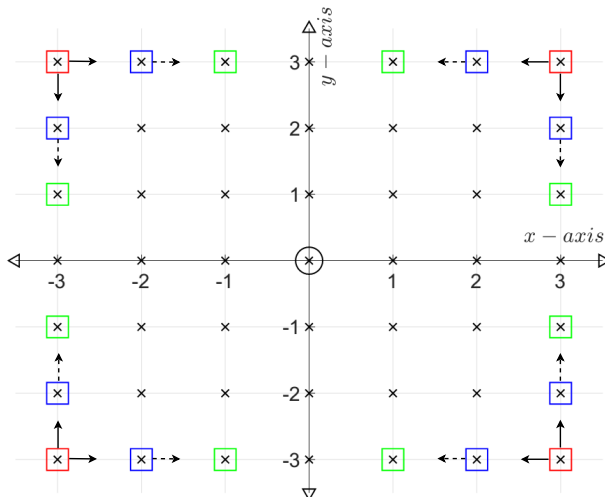


Figure 2: Selection Process for θ_p estimation stage.

Proof. Please see Appendix A. □

Theorem 1 presents the optimal selection strategy when the goal is to minimize $\mathbb{E}_\theta\{CRLB_\theta\}$. This is an extension of our previous work in [3] where we used a greedy algorithm to minimize $\mathbb{E}_\theta\{CRLB_\theta\}$. This strategy itself can be used as an independent selection method. The most important advantage of this method is that the desired set can be determined offline, and there is no need for online calculations, which leads to fast and easy implementation. For the rest of the paper, this method of antenna selection is referred to as *expected* method.

Another important aspect of Theorem 1 is the shape of the selected antennas. When $F \leq 4(M - 1)$, the optimal choice creates four subarrays of antennas. This is in accordance with the same results presented in [20] for large intelligent surfaces, which shows four smaller subarrays perform better than one big antenna array for estimating AoA estimation. We saw the same results in [3] when the greedy algorithm is utilized to select antennas, where the goal is to minimize the $\mathbb{E}_\theta\{CRLB_\theta\}$. Furthermore, we will see in Section VI that for the real-time antenna selection, where the goal is to minimize $CRLB_\theta$, the greedy algorithm will again create smaller subarrays that are separated from one another.

B. Main Antenna selection

In this part, we select the total number of desired antennas based on the θ_p , acquired in the previous step. In this stage, we use a greedy algorithm to minimize the $CRLB_\theta$. Because $CRLB_\theta$

in (9) is for a planar antenna array, the greedy algorithm requires a starting point composed of three antennas selected simultaneously. This means that the first three antennas (the minimum number to form a plane) must be selected together and cannot be selected in a greedy approach. The search for selecting these three antennas together to initiate the greedy algorithm is usually very costly in terms of computational complexity. This is because one has to go through all possible combinations of choosing three antennas over $(M + 1)^2$. However, with the help of the following theorem, this complexity will be reduced to only two possible choices for any M . In the following Theorem, we provide the optimal starting set for the greedy algorithm and prove that this set is the best possible choice. The coordinates of the optimal choices are extracted from the pattern observed in the simulations.

Theorem 2. *The optimal first three antennas that minimizes $CRLB_\theta$ for different values of θ in the first quarter of the trigonometric circle are as the following:*

If $0 \leq \theta \leq \frac{\pi}{4} - \theta_0$,

$$\mathcal{S}_3 = \{(0, 0), (-\frac{M}{2}, \frac{M}{2}), (x_2, \frac{M}{2})\}, \quad (11)$$

where

$$x_2 = \begin{cases} \lfloor \frac{M(1-2\alpha)}{2} \rfloor & \text{if } g_x(\lfloor \frac{M(1-2\alpha)}{2} \rfloor) \leq g_x(\lceil \frac{M(1-2\alpha)}{2} \rceil) \\ \lceil \frac{M(1-2\alpha)}{2} \rceil & \text{if } g_x(\lfloor \frac{M(1-2\alpha)}{2} \rfloor) > g_x(\lceil \frac{M(1-2\alpha)}{2} \rceil), \end{cases}$$

If $\frac{\pi}{4} - \theta_0 < \theta < \frac{\pi}{4} + \theta_1$,

$$\mathcal{S}_3 = \{(0, 0), (-\frac{M}{2}, \frac{M}{2} - 1), (1 - \frac{M}{2}, \frac{M}{2})\}, \quad (12)$$

If $\frac{\pi}{4} + \theta_1 \leq \theta \leq \frac{\pi}{2}$,

$$\mathcal{S}_3 = \{(0, 0), (-\frac{M}{2}, \frac{M}{2}), (-\frac{M}{2}, y_2)\}, \quad (13)$$

where

$$y_2 = \begin{cases} \lfloor \frac{M(2-\alpha)}{2\alpha} \rfloor & \text{if } g_y(\lfloor \frac{M(2-\alpha)}{2\alpha} \rfloor) \leq g_y(\lceil \frac{M(2-\alpha)}{2\alpha} \rceil) \\ \lceil \frac{M(2-\alpha)}{2\alpha} \rceil & \text{if } g_y(\lfloor \frac{M(2-\alpha)}{2\alpha} \rfloor) > g_y(\lceil \frac{M(2-\alpha)}{2\alpha} \rceil), \end{cases}$$

$\alpha = \tan(\theta)$,

$$g_x(x) = \frac{(1 - \alpha)^2 + (\frac{2}{M}x + \alpha)^2}{(\frac{M}{2} + x)^2}, \quad (14)$$

$$g_y(x) = \frac{(1 - \alpha)^2 + (\frac{2\alpha}{M}x - 1)^2}{(\frac{M}{2} - x)^2}, \quad (15)$$

$\theta_0 = \tan^{-1}(x_2)$ and $\theta_1 = \tan^{-1}\left(\frac{M^2(3M^2-6M+2)x_1}{(M-2)(3M-2)(M^2-2M+2)}\right)$ where x_2 and x_1 are the bigger and the smaller root of the following equation (solved for x), respectively

$$\begin{aligned} &M^2(3M^2 - 6M + 2)x^2 - 2M(3M^3 - 10M^2 + 12M - 4)x \\ &+ (M - 2)(3M - 2)(M^2 - 2M + 2) = 0. \end{aligned} \quad (16)$$

Proof. Please see Appendix B. □

Using same procedure the following sets are the optimal start set for other ranges of θ :

$$\text{If } \frac{\pi}{2} < \theta \leq \frac{3\pi}{4} - \theta_0,$$

$$\mathcal{S}_3 = \{(0, 0), \left(\frac{M}{2}, \frac{M}{2}\right), \left(\frac{M}{2}, y_2\right)\}, \quad (17)$$

where

$$y_2 = \begin{cases} \lfloor \frac{-M(2+\alpha)}{2\alpha} \rfloor & \text{if } g_{2,y}(\lfloor \frac{-M(2+\alpha)}{2\alpha} \rfloor) \leq g_{2,y}(\lceil \frac{-M(2+\alpha)}{2\alpha} \rceil) \\ \lceil \frac{-M(2+\alpha)}{2\alpha} \rceil & \text{if } g_{2,y}(\lfloor \frac{-M(2+\alpha)}{2\alpha} \rfloor) > g_{2,y}(\lceil \frac{-M(2+\alpha)}{2\alpha} \rceil), \end{cases}$$

$$\text{If } \frac{3\pi}{4} - \theta_0 < \theta < \frac{3\pi}{4} + \theta_1,$$

$$\mathcal{S}_3 = \{(0, 0), \left(\frac{M}{2}, \frac{M}{2} - 1\right), \left(\frac{M}{2} - 1, \frac{M}{2}\right)\}, \quad (18)$$

$$\text{If } \frac{3\pi}{4} + \theta_1 \leq \theta < \pi,$$

$$\mathcal{S}_3 = \{(0, 0), \left(\frac{M}{2}, \frac{M}{2}\right), (x_2, \frac{M}{2})\}, \quad (19)$$

where

$$x_2 = \begin{cases} \lfloor \frac{-M(1+2\alpha)}{2} \rfloor & \text{if } g_{2,x}(\lfloor \frac{-M(1+2\alpha)}{2} \rfloor) \leq g_{2,x}(\lceil \frac{-M(1+2\alpha)}{2} \rceil) \\ \lceil \frac{-M(1+2\alpha)}{2} \rceil & \text{if } g_{2,x}(\lfloor \frac{-M(1+2\alpha)}{2} \rfloor) > g_{2,x}(\lceil \frac{-M(1+2\alpha)}{2} \rceil), \end{cases}$$

$$g_{2,x}(x) = \frac{(1 + \alpha)^2 + (\frac{2}{M}x + \alpha)^2}{(\frac{M}{2} - x)^2}, \quad (20)$$

$$g_{2,y}(x) = \frac{(1 + \alpha)^2 + (\frac{2\alpha}{M}x + 1)^2}{(\frac{M}{2} - x)^2}. \quad (21)$$

For $\pi < \theta \leq \frac{5\pi}{4} - \theta_0$, $\frac{5\pi}{4} - \theta_0 < \theta < \frac{5\pi}{4} + \theta_1$, $\frac{5\pi}{4} + \theta_1 \leq \theta < \frac{3\pi}{2}$, $\frac{3\pi}{2} < \theta \leq \frac{7\pi}{4} - \theta_0$, $\frac{7\pi}{4} - \theta_0 < \theta < \frac{7\pi}{4} + \theta_1$ and $\frac{7\pi}{4} + \theta_1 \leq \theta < 2\pi$ the optimal choices are exactly same as the ones for $0 < \theta \leq \frac{\pi}{4} - \theta_0$, $\frac{\pi}{4} - \theta_0 < \theta < \frac{\pi}{4} + \theta_1$, $\frac{\pi}{4} + \theta_1 \leq \theta < \frac{\pi}{2}$, $\frac{\pi}{2} < \theta \leq \frac{3\pi}{4} - \theta_0$, $\frac{3\pi}{4} - \theta_0 < \theta < \frac{3\pi}{4} + \theta_1$ and $\frac{3\pi}{4} + \theta_1 \leq \theta < \pi$, respectively.

By virtue of Theorem 2, the choice of the first three antennas for any M is reduced to only two sets. For example, if we have an array of 81 antennas, the total number of possible sets for

the start point is $\binom{80}{2} = 3160$ cases. Such a search pool can prevent the antenna selection in real-time, but with the help of Theorem 2, this problem is solved. Now that we have optimal starting point for the greedy algorithm, by using the characteristics of the $CRLB_\theta$ formulation it is possible to reduce the search area of the greedy algorithm to half.

Corollary 2.1. *Every antenna selected in the Main Stage, either for the start set or by the greedy algorithm, has the same contribution in the $CRLB_\theta$ as its reciprocal counterpart w.r.t the reference point and can be replaced with it.*

Proof. Consider that in the n th step of the greedy algorithm if $(-x_1, -y_1)$ is added instead of (x_1, y_1) . By noting the formulation of $U(s)$, at the nominator all the elements of both $\tilde{\Sigma}_1$ and $\tilde{\Sigma}_2$ are squared before addition. So, all x and y elements are squared and changing the sign of those elements will not affect the nominator. In the denominator, again the $tr(\tilde{\Sigma}_1^2)tr(\tilde{\Sigma}_2^2)$ will not be affected due to the fact that their elements are squared. For $tr(\tilde{\Sigma}_1\tilde{\Sigma}_1)$, each x is multiplied by its corresponding y , so if the sign of both of them are changed simultaneously, the final result will not change. \square

By virtue of the Corollary 2.1, the search area of the greedy algorithm will be restricted only to the half of the antenna array. This is because when the contribution of the antennas in the first half is calculated, the contribution of all of the antennas at the other half will be same as the first one. This significantly reduces the computational complexity of the greedy algorithm that is essential for the real-time utilization. The complete procedure of the real-time antenna selection algorithm is presented in Table. I.

In certain applications where the AoA of a UT is being tracked like [21], [22], the preliminary stage of the antenna selection can be ignored. Suppose the frequency of tracking estimation is fast enough that AoA of the UT is not hugely changed. In that case, based on previous estimation of the UT's AoA, the system has a fair idea of the current AoA. So, the preliminary estimation stage can be removed, and θ_p can be replaced with the estimation of the previous AoA. This will help such applications to implement the real-time antenna selection with even lower computational complexity.

Remark 2. *From (9), (10) and (31) it is evident that changing the channel model does not affect the configuration of selected antennas. Indeed, changing the channel model to consider path-loss signals will only change the $|h_d|^2$ coefficient in the aforementioned equations [3]. So,*

get F_p, F	
Select F_p antennas based on Theorem1. Estimate θ_p .	Preliminary Stage
Using θ_p , select \mathcal{S}_3 based on Theorem2. $\mathcal{S} := \mathcal{S}_3$ For $f := 4$ to F do For $x := 0$ to $M/2$ do For $y := 0$ to $M/2$ do If $(x, y) \notin \mathcal{S}$ do $\mathcal{S}(f) := (x, y)$ $\mathbf{V}(x, y) := CRLB_\theta(\mathcal{S})$ EndIf EndFor EndFor $\mathcal{S}(f) := \arg \min_{(x,y)} \mathbf{V}$ EndFor return \mathcal{S}	Main Stage

Table I: Real-time antenna selection algorithm.

the presented antenna selection methods can be implemented in any channel model.

V. MULTI-USER SCENARIO

In this section, we generalize the real-time antenna selection method for the multi-user scenario, where K number of UTs use same time and frequency slots to transmit their pilot signals to the BS. As the cost function of the expected method do not consider the actual values of AoAs, it can be implemented in the multi-user scenario without any change. So, we only focus on the real-time antenna selection method.

The first major change in the multi-user scenario is that $CRLB_\theta$ for all UTs will become a diagonal matrix whose (k, k) th element will be $CRLB_{\theta_k}$ as in (9) where θ_k is the AoA of k th UT [3]. Because all of the UTs have same priority to be localized, the cost function of the system will be summation of the $CRLB_{\theta_k}$ s for all UTs.

Due to the fact that pilots of all UTs are sent at the same time and frequency, when the system wants to estimate θ_p , the difference in phase in the aggregated receive signal will be sum of individual phase differences caused by each UT. In this case, if $F_p \leq K$, the system

can only estimate the average of all of AoAs. This is because the phase differences of pilots from different UTs will add up (either constructively or destructively) and system will not be able to distinguish them. When $F_p > K$, although it is possible to estimate all of AoAs, it will require relatively more sophisticated methods (like MUSIC algorithm). These methods usually demand many snapshots and computational resources that are reserved for the main estimation procedure.

The method we propose in this case is to estimate the average of all AoAs, and select the antennas, according to this value. For example, if we have three UTs at $\frac{\pi}{10}$, $\frac{\pi}{6}$ and $\frac{\pi}{3}$, (assuming BS knows the number of UTs) the average is $\frac{\pi}{5}$. After obtaining the average AoA, the system continues the antenna selection same as the single UT case by putting the average AoA as the θ_p .

VI. NUMERICAL RESULTS

In this section, we test the presented theorems by Monte-Carlo simulations. As a benchmark, the performance of real-time antenna selection is compared with expected antenna selection method. In the expected method, only the preliminary stage of the proposed antenna selection is used (also related to our work previous work [3]). Also, we compare both of selection methods with a strategy in which the preliminary stage is done, but the start point of the greedy algorithm is randomly selected and θ_p is only used in the greedy algorithm's cost function (i.e. Theorem2 is not used)³. In the following figures, $\frac{d}{\lambda} = 0.5$, $|h_d|^2 = 1$, $\rho = 0dB$ and $\varphi = \frac{\pi}{3}$.

Fig. 3 shows the $CRLB_\theta$ for all possible AoAs when only three antennas are selected, using different methods for $M = 6$. The red curve is $CRLB_\theta$ when three antennas are selected to minimize $\mathbb{E}_\theta\{CRLB_\theta\}$. The blue and green curves are the result of selecting antennas to minimize $CRLB_\theta$, using Theorem 2 and global search, respectively. Moreover, the dotted lines show $\theta_0 = 43.1352^\circ$ and $\theta_1 = 46.8648^\circ$, where the optimal choices change according to (12) and (16). It is seen that Theorem 2 is perfectly capable of predicting the optimal set for the first three antennas.

Fig. 4 indicates the resulted $CRLB_\theta$ versus θ for different antenna selection strategies and scenarios. In this figure, $M = 6$ and $F = 13$. The magenta curve results when antennas are

³We do not compare our results with total random selection method (in which all of antennas are selected randomly) as it performs so poorly that it distorts the scale of plots. In current view one can better appreciate small differences in different selection methods.

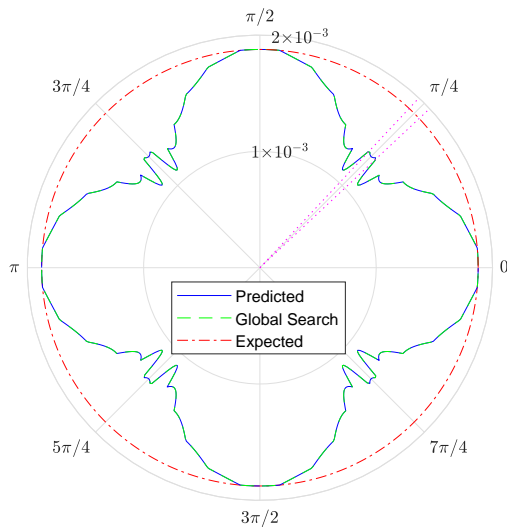


Figure 3: $CRLB_\theta$ versus θ for $F = 3$ and different selection methods.

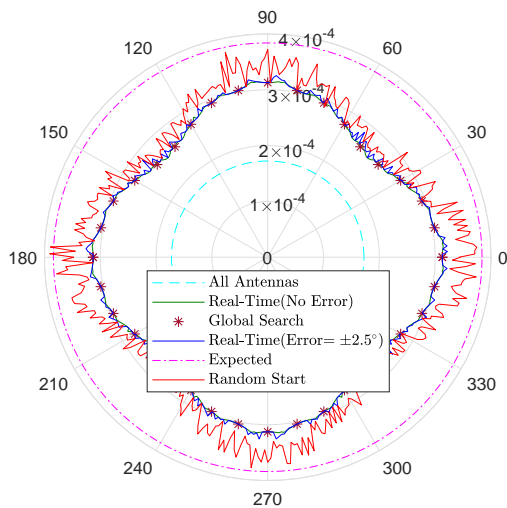


Figure 4: $CRLB_\theta$ versus θ for $F = 13$ different selection strategies and scenarios.

selected to minimize $\mathbb{E}_\theta\{CRLB_\theta\}$. The cyan curve is for the case when all of the available antennas are used ($F = (M + 1)^2$). The green curve results from the real-time greedy method, when AoA is perfectly known, i.e., $\theta_p = \text{AoA}$. It is seen that the real-time antenna selection method secures between 52% and 68% of total performance (depending on the value of θ), only by using a quarter of total available antennas. Moreover, using the expected antenna selection method, 45% of total performance is achieved. The star markers (*) show the $CRLB_\theta$ that is obtained through global search, i.e., the global minimum for $F = 13$. It is seen that the

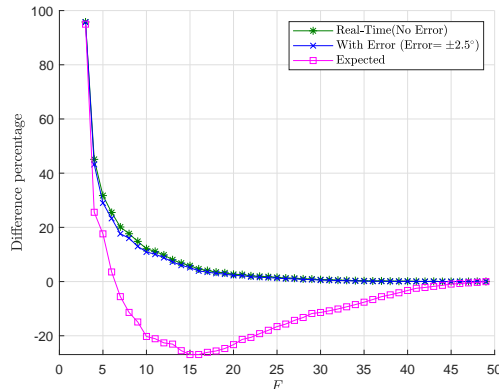


Figure 5: Performance improvement percentage of different methods relative to real-time method with random start point.

greedy algorithm obtains a very close performance to global search with much less computational complexity, indicating that the greedy algorithm with optimal start point is a reasonable choice for antenna selection. In the blue curve, constant noise is added to the θ_p to show how the selection strategy performs when $\theta_p \neq \text{AoA}$. The noise value is 2.5° with a random positive or negative sign, i.e., $\theta_p = \text{AoA} \pm 2.5^\circ$. It should be noted that the $CRLB_\theta$ is in the order of 3×10^{-4} ($\approx 0.01^\circ$), and the added error is more than two orders of magnitude higher than $CRLB_\theta$. It is seen that even with this amount of error, the selection process is performing so close to the optimal case. Also, this curve shows that different AoAs have different tolerances against error in θ_p . It should be noted that an error in θ_p affects both parts of the real-time selection algorithm, the start set, and the greedy part. This amount of error tolerancy can motivate one to create a look-up table for the real-time antenna selection by selecting a set for every 2.5° (or any other value) and using a proper set according to the value of θ_p to extremely simplify the antenna selection procedure. The red curve with a random start set is plotted to see the effects of the optimal start set. In this curve, the optimal start set that is proposed by Theorem2 is not used, and instead, two random antennas are selected in addition to the reference point. The greedy part is the same as the blue curve, and θ_p is used in the greedy part of the red curve. It is seen that, in general, $CRLB_\theta$ deteriorates when the optimal start point is not used, sometimes even worse than the expected method. This highlights the importance of the optimal start point, presented in Theorem2.

Fig. 5 shows the relative advantage of real-time and expected antenna selection methods to

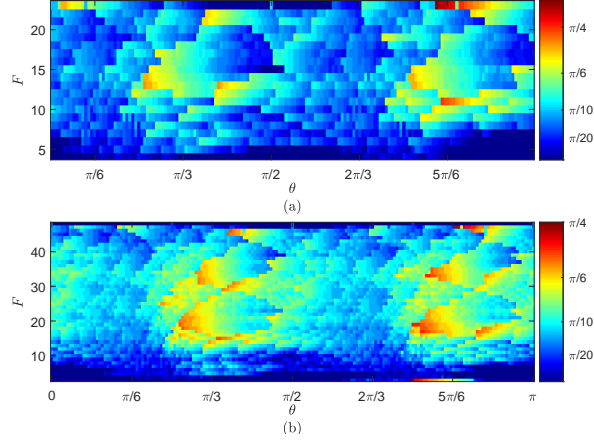


Figure 6: Error tolerancy of real-time antenna selection strategy for: (a) $M = 4$ and (b) $M = 6$.

the selection method in which only the start point is selected randomly, i.e., θ_p is only used in the greedy part. For all curves, each point is calculated as $\frac{\sum_{\theta=0}^{2\pi} ([CRLB_{\theta}]_R - [CRLB_{\theta}]_A)}{N \sum_{\theta=0}^{2\pi} [CRLB_{\theta}]_R}$, where $[CRLB_{\theta}]_A$ means the $CRLB_{\theta}$ resulted by using method A , and A can be real-time (either with or without error) or expected method, $[CRLB_{\theta}]_R$ means the $CRLB_{\theta}$ resulted by using real-time method with random start point and N is total number of angles that have been summed. This figure aims to show that for every F , how using proposed methods, namely real-time with optimal start point, increases the performance w.r.t the case in which the real-time method is utilized but with the random start point. It is seen that when F is relatively small, by using the presented optimal start set, the performance increases significantly. As F grows, the difference in performance decreases. This is because as more and more antennas are selected, even if the start set is selected randomly, other antennas that are selected in the greedy section by the random algorithm will make up a considerable portion of the total selected antennas. So the contribution of two antennas that are optimally selected for the start set will decrease. Therefore, as more antennas are selected, the importance of the optimal start set reduces because antennas with high contributions will be selected one way or another. Another point of Fig. 5 is the behavior of the curve for the expected antenna selection method. First, it has a positive relative performance. Then it becomes negative, meaning that for certain F expected method is better than the real-time with a random start point, and as F increases, the real-time approach, even with random start point, is better than the expected method.

Fig. 6 is plotted to further examine how the main real-time antenna selection method (the one

that takes advantage of optimal start set) performs compared to the expected method. This figure represents how error tolerant the real-time antenna selection is, compared with the expected antenna selection method. In this figure, the x-axis is the AoA, and the y-axis is the number of selected antennas. For each point in this 2D plane, the color indicates how much error the real-time algorithm can bear in the preliminary stage and still have lower $CRLB_\theta$ than the antenna selection method that minimizes expected $CRLB_\theta$. Deep blue color means lower error tolerancy, and the more the color of a point becomes reddish, the higher amount of error can be tolerated by the real-time algorithm. It is seen that starting after $\frac{\pi}{3}$ up to around $\frac{\pi}{2}$, between $5 \leq F \leq 20$ for $M = 4$ and between $10 \leq F \leq 40$ for $M = 6$, the real-time algorithm shows its highest resistance. Moreover, by increasing the total number of antennas, the real-time algorithm becomes more error tolerant. This means that the real-time selection method performs very well when F is around half of the M , i.e., for relatively moderate F . Also, it should be noted that the reason for the low error tolerancy in higher values of F is that as most of antennas are already selected by both selection strategies, the $CRLB_\theta$ is reaching its final value (that is using $(M + 1)^2$ antennas) and then even selecting one antenna with lower priority results in a very small but higher value for $CRLB_\theta$, so error tolerancy is low. However, despite lower tolerancy, the value of resulted $CRLB_\theta$ is very close for both strategies.

In Fig. 7, the inverse product of F and $CRLB_\theta$ is plotted for $M = 6$ and $M = 4$ to show how efficient each selection strategy is using its selected antennas. This can be seen as a basic study and can be modified for any kind of efficiency study, like localization efficiency that is introduced in our previous work [4]. In this figure, in both real-time and expected selection methods for each F , the average value for all possible θ s are plotted, i.e. $\frac{1}{N} \sum_{\theta=0}^{2\pi} CRLB_\theta$ where N is total number of θ s that are summed. It is seen that the real-time selection method always obtains higher efficiency in terms of antenna usage. As expected from Fig. 6, the region that real-time selection has the highest efficiency difference w.r.t the expected antenna selection corresponds to the same region that real-time selection has higher error tolerancy, as well. Also, noting that the endpoint of the curves indicate the efficiency of antenna usage without antenna selection, by making use of antenna selection significantly higher efficiencies can be obtained.

Finally, in Fig. 8 an example of the selected antennas by the presented algorithms for $M = 6$, $F = 20$ and $\theta = \frac{\pi}{3}$ is plotted. In this figure, square markers show the selected antennas by the real-time antenna selection (without error). The blue squares indicate start points for the greedy algorithm, and the greedy algorithm selected magenta ones. Also, green circles demonstrate the

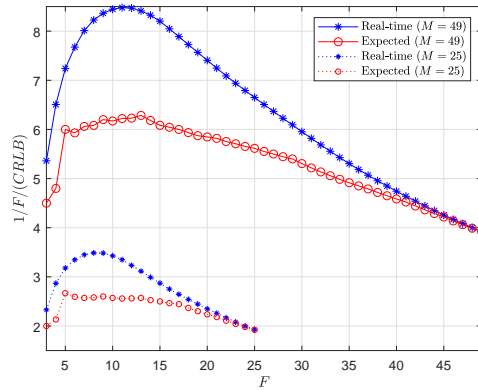


Figure 7: The inverse of the product of $CRLB$ and F , versus F .

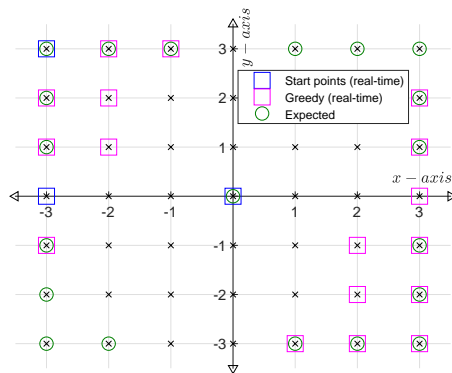


Figure 8: Selected antennas by both real-time and expected algorithms for $F = 20$ and $\theta = \frac{\pi}{3}$.

selected antennas by the expected algorithm. We observe that the greedy algorithm creates two separate subarrays to estimate AoA. This result that several smaller subarrays perform better than one big array is reported also for large intelligent surfaces in [20] and Massive MIMO systems in [3]. Our results for both expected and real-time antenna selection methods are in accordance with these results.

VII. CONCLUSION

In this paper, we studied antenna selection for AoA estimation for a square planar antenna array. We proposed two CRLB based antenna selection methods for AoA estimation. In the first method, motivated by our previous studies, the goal is to minimize the expected value of the $CRLB_{\theta}$. The expectation is used to remove the dependency of $CRLB_{\theta}$ to the actual value of

the AoA. This is because there is no knowledge about AoA before its estimation, except its range and distribution. The optimal strategy for antenna selection in this scenario is presented.

Next, using the first introduced antenna selection method, a two-step real-time antenna selection method is developed. In this method, an initial set of antennas are selected to minimize the expected $CRLB_\theta$. By using this set, a fast and crude estimation of AoA is done. Then the estimated AoA is used in a greedy algorithm whose objective function is to minimize the $CRLB_\theta$. To make the algorithm fast enough (so it can be run in real-time), the optimal start point of the algorithm is presented. Moreover, a corollary that reduces the search space to almost half of the available antennas is presented to reduce the algorithm's computational complexity.

Numerical results show a considerable gain of performance when either one of the methods is employed. Also, it is shown that greedy algorithm with optimal starting point obtains quite close performance to global search. Furthermore, both presented algorithms' error tolerancy and efficiency of antenna usage are compared with one another and with the real-time method whose start point is random. It is seen that when the number of active antennas is moderate, the real-time antenna selection (with optimal start point) has its highest error tolerancy and efficiency w.r.t the antenna selection method that aims to minimize expected $CRLB_\theta$. On the other hand, when the number of selected antennas is close to the total number of available antennas, the antenna selection to minimize expected $CRLB_\theta$ obtains very close performance.

VIII. ACKNOWLEDGMENT

This work is supported by F.R.S.-FNRS under the EOS research project MUSEWINET (EOS project 30452698).

REFERENCES

- [1] H. Wymeersch, G. Seco-Granados, G. Destino, D. Dardari, and F. Tufvesson, "5g mmwave positioning for vehicular networks," *IEEE Wireless Communications*, vol. 24, no. 6, pp. 80–86, 2017.
- [2] A. Shahmansoori, G. E. Garcia, G. Destino, G. Seco-Granados, and H. Wymeersch, "Position and orientation estimation through millimeter-wave mimo in 5g systems," *IEEE Transactions on Wireless Communications*, vol. 17, no. 3, pp. 1822–1835, 2017.
- [3] M. Arash, H. Mirghasemi, I. Stupia, and L. Vandendorpe, "Analysis of crlb for aoa estimation in massive mimo systems," in *2021 IEEE 32nd Annual International Symposium on Personal, Indoor and Mobile Radio Communications (PIMRC)*, pp. 1395–1400, IEEE, 2021.
- [4] M. Arash, H. Mirghasemi, I. Stupia, and L. Vandendorpe, "Localization efficiency in massive mimo systems," *arXiv preprint arXiv:2003.07978*, 2020.

- [5] Q. Li, T. Su, and K. Wu, "Accurate doa estimation for large-scale uniform circular array using a single snapshot," *IEEE Communications Letters*, vol. 23, no. 2, pp. 302–305, 2019.
- [6] A. Hu, T. Lv, H. Gao, Z. Zhang, and S. Yang, "An esprit-based approach for 2-d localization of incoherently distributed sources in massive mimo systems," *IEEE Journal of Selected Topics in Signal Processing*, vol. 8, no. 5, pp. 996–1011, 2014.
- [7] N. H. M. Adnan, I. M. Rafiqul, and A. Z. Alam, "Effects of inter element spacing on large antenna array characteristics," in *2017 IEEE 4th International Conference on Smart Instrumentation, Measurement and Application (ICSIMA)*, pp. 1–5, IEEE, 2017.
- [8] E. Björnson, L. Sanguinetti, H. Wymeersch, J. Hoydis, and T. L. Marzetta, "Massive mimo is a reality—what is next?: Five promising research directions for antenna arrays," *Digital Signal Processing*, vol. 94, pp. 3–20, 2019.
- [9] C. Huang, G. C. Alexandropoulos, A. Zappone, M. Debbah, and C. Yuen, "Energy efficient multi-user miso communication using low resolution large intelligent surfaces," in *2018 IEEE Globecom Workshops (GC Wkshps)*, pp. 1–6, IEEE, 2018.
- [10] M. Arash, E. Yazdian, M. S. Fazel, G. Brante, and M. A. Imran, "Employing antenna selection to improve energy efficiency in massive mimo systems," *Transactions on Emerging Telecommunications Technologies*, vol. 28, no. 12, p. e3212, 2017.
- [11] A. M. Elbir and K. V. Mishra, "Joint antenna selection and hybrid beamformer design using unquantized and quantized deep learning networks," *IEEE Transactions on Wireless Communications*, vol. 19, no. 3, pp. 1677–1688, 2019.
- [12] A. S. Khan, I. Chatzigeorgiou, S. Lambotharan, and G. Zheng, "Network-coded noma with antenna selection for the support of two heterogeneous groups of users," *IEEE Transactions on Wireless Communications*, vol. 18, no. 2, pp. 1332–1345, 2019.
- [13] H. Godrich, A. P. Petropulu, and H. V. Poor, "Sensor selection in distributed multiple-radar architectures for localization: A knapsack problem formulation," *IEEE Transactions on Signal Processing*, vol. 60, no. 1, pp. 247–260, 2011.
- [14] S. Mulleti, C. Saha, H. S. Dhillon, and Y. C. Eldar, "A fast-learning sparse antenna array," in *2020 IEEE Radar Conference (RadarConf20)*, pp. 1–6, IEEE, 2020.
- [15] A. Bhattacharya, C. Zhan, A. Maji, H. Gupta, S. R. Das, and P. M. Djurić, "Selection of sensors for efficient transmitter localization," *IEEE/ACM Transactions on Networking*, 2021.
- [16] H. Zhang, J. Shi, Q. Zhang, B. Zong, and J. Xie, "Antenna selection for target tracking in colocated mimo radar," *IEEE Transactions on Aerospace and Electronic Systems*, vol. 57, no. 1, pp. 423–436, 2020.
- [17] X. Wang, E. Aboutanios, and M. G. Amin, "Adaptive array thinning for enhanced doa estimation," *IEEE Signal Processing Letters*, vol. 22, no. 7, pp. 799–803, 2014.
- [18] E. Aboutanios, H. Nosrati, and X. Wang, "Online antenna selection for enhanced doa estimation," in *ICASSP 2021-2021 IEEE International Conference on Acoustics, Speech and Signal Processing (ICASSP)*, pp. 8468–8472, IEEE, 2021.
- [19] J. M. Romero-Jerez and A. J. Goldsmith, "Performance of multichannel reception with transmit antenna selection in arbitrarily distributed nagakami fading channels," *IEEE Transactions on Wireless Communications*, vol. 8, no. 4, pp. 2006–2013, 2009.
- [20] S. Hu, F. Rusek, and O. Edfors, "Beyond massive mimo: The potential of positioning with large intelligent surfaces," *IEEE Transactions on Signal Processing*, vol. 66, no. 7, pp. 1761–1774, 2018.
- [21] X. Li, E. Leitinger, M. Oskarsson, K. Åström, and F. Tufvesson, "Massive mimo-based localization and mapping exploiting phase information of multipath components," *IEEE transactions on wireless communications*, vol. 18, no. 9, pp. 4254–4267, 2019.
- [22] M. Zhu, J. Vieira, Y. Kuang, K. Åström, A. F. Molisch, and F. Tufvesson, "Tracking and positioning using phase information from estimated multi-path components," in *2015 IEEE International Conference on Communication Workshop (ICCW)*, pp. 712–717, IEEE, 2015.

APPENDIX A
PROOF OF THEOREM 1

The process of proof is to show that for every step, the presented set in Theorem1 obtains lowest possible value for $U(\mathcal{S})$. We show this for the first two steps, i.e. for $F_p \leq 5$ and $5 < F_p \leq 13$. The rest of the proof is exactly same as these steps and can be simply repeated until any arbitrary F_p .

For $F_p = 5$, selecting \mathcal{S}_{p_1} will result in $U(\mathcal{S}_{p_1}) = \frac{2}{M^2}$. Now we show that any other set than \mathcal{S}_{p_1} , results in higher value for $U(\mathcal{S})$. Assume any $\bar{\mathcal{S}}_{p_1} = \{(0, 0), (x_1, y_1), (x_2, y_2), (x_3, y_3), (x_4, y_4)\}$ to be a set of antennas which at least has one different antenna from \mathcal{S}_{p_1} , we have

$$U(\bar{\mathcal{S}}_{p_1}) = \frac{\sum_{i=1}^5 (x_i^2 + y_i^2)}{(\sum_{i=1}^5 x_i^2)(\sum_{i=1}^5 y_i^2) - (\sum_{i=1}^5 x_i y_i)^2}. \quad (22)$$

Because at least one antenna in $\bar{\mathcal{S}}_{p_1}$ has at least one different coordinate from the antennas in the \mathcal{S}_{p_1} , so at least either $\sum_{i=1}^5 x_i^2 < M^2$ or $\sum_{i=1}^5 y_i^2 < M^2$, so

$$\begin{aligned} (M^2 - \sum_{i=1}^5 y_i^2) \sum_{i=1}^5 x_i^2 + (M^2 - \sum_{i=1}^5 x_i^2) \sum_{i=1}^5 y_i^2 &= M^2 \sum_{i=1}^5 (x_i^2 + y_i^2) - 2(\sum_{i=1}^5 x_i^2)(\sum_{i=1}^5 y_i^2) > 0 \\ &\geq -2(\sum_{i=1}^5 x_i y_i)^2. \end{aligned} \quad (23)$$

Therefore

$$M^2 \sum_{i=1}^5 x_i^2 + y_i^2 > 2((\sum_{i=1}^5 x_i^2)(\sum_{i=1}^5 y_i^2) - (\sum_{i=1}^5 x_i y_i)^2). \quad (24)$$

By noting that $(\sum_{i=1}^5 x_i^2)(\sum_{i=1}^5 y_i^2) - (\sum_{i=1}^5 x_i y_i)^2 > 0$ due to Cauchy-Schwarz inequality, we obtain

$$\frac{\sum_{i=1}^5 (x_i^2 + y_i^2)}{(\sum_{i=1}^5 x_i^2)(\sum_{i=1}^5 y_i^2) - (\sum_{i=1}^5 x_i y_i)^2} > \frac{2}{M^2}. \quad (25)$$

When, $3 < F_p < 5$, all of greater signs ($>$) in (23)-(25) will be replaced with the greater or equal sign (\geq), with equality happening for any two subsets of \mathcal{S}_{p_1} .

For $F_p = 13$, the antennas set of \mathcal{S}_{p_2} will result in $U(\mathcal{S}_{p_1} \cup \mathcal{S}_{p_2}) = \frac{2}{2M^2 + 4(\frac{M}{2} - 1)^2}$. For this set, $\sum_{i=1}^5 x_i^2 = \sum_{i=1}^5 y_i^2 = 2M^2 + 4(\frac{M}{2} - 1)^2$. We call $\bar{\mathcal{S}}_{p_2}$ a set in which at least one of the coordinates of one antenna is different from the $\mathcal{S}_{p_1} \cup \mathcal{S}_{p_2}$. In this case, depending on the fact that which coordinate is different, three scenarios will happen. First scenario is that either $\sum_{i=1}^5 x_i^2$ or $\sum_{i=1}^5 y_i^2$ is reduced and the other one remains constant. Second scenario is when both of them are reduced and the third scenario is when one is increased and the other one is

reduced. It should be noted that no other choice for first 13 antenna other than antennas in \mathcal{S}_{p_2} can simultaneously increase both $\sum_{i=1}^5 x_i^2$ and $\sum_{i=1}^5 y_i^2$. This is because expect the reference point, all of antennas in \mathcal{S}_{p_2} are the ones whose x_i s and y_i s are simultaneously maximized.

In the aforementioned scenarios, the values of $\sum_{i=1}^5 x_i^2$ and $\sum_{i=1}^5 y_i^2$ for \mathcal{S}_{p_2} will change to

$$\begin{aligned}\sum_{i \in \mathcal{S}_{p_2}} x_i^2 &= 2M^2 + 4\left(\frac{M}{2} - 1\right)^2 - a, \\ \sum_{i \in \mathcal{S}_{p_2}} y_i^2 &= 2M^2 + 4\left(\frac{M}{2} - 1\right)^2 - b,\end{aligned}\tag{26}$$

We have

$$\begin{aligned}& (2M^2 + 4\left(\frac{M}{2} - 1\right)^2) \left(\sum_{i \in \bar{\mathcal{S}}_{p_2}} x_i^2 + y_i^2 \right) - 2 \left(\sum_{i \in \bar{\mathcal{S}}_{p_2}} x_i^2 \right) \left(\sum_{i \in \bar{\mathcal{S}}_{p_2}} y_i^2 \right) \\ &= (2M^2 + 4\left(\frac{M}{2} - 1\right)^2) \left(\sum_{i \in \mathcal{S}_{p_2}} x_i^2 + y_i^2 - a - b \right) - 2 \left(\sum_{i \in \mathcal{S}_{p_2}} x_i^2 - a \right) \left(\sum_{i \in \mathcal{S}_{p_2}} y_i^2 - b \right) \\ &= (2M^2 + 4\left(\frac{M}{2} - 1\right)^2) \left(\sum_{i \in \mathcal{S}_{p_2}} x_i^2 + y_i^2 \right) - 2 \left(\sum_{i \in \mathcal{S}_{p_2}} x_i^2 \right) \left(\sum_{i \in \mathcal{S}_{p_2}} y_i^2 \right) + (2M^2 \\ &+ 4\left(\frac{M}{2} - 1\right)^2)(a + b) - 2ab \\ &= \underbrace{\left(2M^2 + 4\left(\frac{M}{2} - 1\right)^2 - \sum_{i \in \mathcal{S}_{p_2}} y_i^2 \right)}_{=0} \sum_{i \in \mathcal{S}_{p_2}} x_i^2 + \underbrace{\left(2M^2 + 4\left(\frac{M}{2} - 1\right)^2 - \sum_{i \in \mathcal{S}_{p_2}} x_i^2 \right)}_{=0} \sum_{i \in \mathcal{S}_{p_2}} y_i^2 \\ &+ (2M^2 + 4\left(\frac{M}{2} - 1\right)^2)(a + b) - 2ab.\end{aligned}\tag{27}$$

Now, (27) is a linear equation w.r.t a and b . Its derivative w.r.t a is

$$2M^2 + 4\left(\frac{M}{2} - 1\right)^2 - 2b,\tag{28}$$

and (28) is always positive because the maximum value of b is $4\left(\frac{M^2}{4}\right)$. So, the slop of (27) is always positive. The most negative value of a happens when all of four antennas with $x = \frac{M}{2} - 1$ in \mathcal{S}_{p_1} are replaced with $\frac{M}{2}$ in $\bar{\mathcal{S}}_{p_1}$. This replacement will result in $a = 4\left(\left(\frac{M}{2} - 1\right)^2 - \left(\frac{M}{2}\right)^2\right)$ and $b = 4\left(\left(\frac{M}{2}\right)^2 - \left(\frac{M}{2} - 2\right)^2\right)$. Therefore, $a + b > 0$ in the most negative value of a . So, a starts from

a positive value with a positive slope, meaning that (27) is positive for every possible value of a . Same thing can be shown w.r.t b . Therefore,

$$\begin{aligned} & (2M^2 + 4(\frac{M}{2} - 1)^2) \left(\sum_{i \in \bar{\mathcal{S}}_{p_2}} x_i^2 + y_i^2 \right) - 2 \left(\sum_{i \in \bar{\mathcal{S}}_{p_2}} x_i^2 \right) \left(\sum_{i \in \bar{\mathcal{S}}_{p_2}} y_i^2 \right) \\ &= (2M^2 + 4(\frac{M}{2} - 1)^2 - b)a + (2M^2 + 4(\frac{M}{2} - 1)^2 - a)b > 0 \geq -2 \left(\sum_{i \in \bar{\mathcal{S}}_{p_2}} x_i y_i \right)^2. \end{aligned} \quad (29)$$

So, for any $\bar{\mathcal{S}}_{p_2}$ we have

$$\frac{\sum_{i=1}^{13} x_i^2 + y_i^2}{\left(\sum_{i=1}^{13} x_i^2 \right) \left(\sum_{i=1}^{13} y_i^2 \right) - \left(\sum_{i=1}^{13} x_i y_i \right)^2} > \frac{2}{\left(2M^2 + 4(\frac{M}{2} - 1)^2 \right)^2}. \quad (30)$$

If $5 < F_p < 13$, all of the greater signs ($>$) in (29) and (30) will be replaced by greater or equal sign (\geq), with equality happening for any two subsets of $\mathcal{S}_{p_1} \cup \mathcal{S}_{p_2}$.

For $14 \leq F < 21$ and other steps the proof is exactly same as $5 < F_p \leq 13$. When all of antennas in the outer most rectangle are selected, then the proof of the next step that is the selection of the four antennas at the corner of the second most outer rectangle, is same as $F_p \leq 5$. Then the process of rest antennas in the same rectangle is same as $5 < F_p \leq 13$, and so on. This process can be repeated for any desired F_p .

APPENDIX B

PROOF OF THEOREM 2

As the main reference for the system, the antenna that is considered as the reference point has to be in the selected set. Then, the $CRLB_\theta$ for any set of three selected antennas $\{(0, 0), (x_1, y_1), (x_2, y_2)\}$, will have the following form

$$CRLB_{\theta,3} = A \times \underbrace{\left(\frac{(x_1 + \alpha y_1)^2 + (x_2 + \alpha y_2)^2}{(x_1 y_2 - x_2 y_1)^2} \right)}_{Q_\theta(x_1, y_1, x_2, y_2)}, \quad (31)$$

where $A = \frac{\cos^2(\theta)}{2\rho_k \beta^2 |h_d|^2 \sin^2(\varphi)}$ and it is independent from selected antennas. So, $Q_\theta(x_1, y_1, x_2, y_2)$ should be minimized with respect to (w.r.t) x_1, y_1, x_2 and y_2

$$\min_{x_1, y_1, x_2, y_2} Q_\theta(x_1, y_1, x_2, y_2), \quad (32a)$$

$$s.t. \quad x_1, y_1, x_2, y_2 \in \left\{ -\frac{M}{2}, \dots, 0, \dots, \frac{M}{2} \right\}, \quad (32b)$$

$$(x_1, y_1) \neq (ax_2, ay_2) \quad for \quad a \in \mathbb{R}, \quad (32c)$$

$$(x_1, y_1) \neq (0, 0), \quad (x_2, y_2) \neq (0, 0), \quad (32d)$$

where (32c) and (32d) ensure that an antenna is not selected twice, and three selected antennas do not compose a line.

For $0 < \theta \leq \frac{\pi}{4} - \theta_0$, first we relax the integer constraint only on x_2 and prove that any other choice than $(x_1^*, y_1^*, x_2^*, y_2^*) = (-\frac{M}{2}, \frac{M}{2}, \frac{M(1-2\alpha)}{2}, \frac{M}{2})$ results in higher $Q_\theta(x_1, y_1, x_2, y_2)$. Then the problem boils down to the choice between two upper and lower integers in the vicinity of x_2 , that can be efficiently solved by directly checking which one results in lower value for $Q_\theta(x_1, y_1, x_2, y_2)$.

By replacing $(x_1^*, y_1^*, x_2^*, y_2^*) = (-\frac{M}{2}, \frac{M}{2}, \frac{M(1-2\alpha)}{2}, \frac{M}{2})$ in Q_θ , we have

$$Q_\theta(x_1^*, y_1^*, x_2^*, y_2^*) = \frac{2}{M^2}. \quad (33)$$

Now we show that for any combination of (x_1, y_1, x_2, y_2) ,

$$\frac{(x_1 + \alpha y_1)^2 + (x_2 + \alpha y_2)^2}{(x_1 y_2 - x_2 y_1)^2} \geq \frac{2}{M^2}. \quad (34)$$

By multiplying both sides of (34) by $M^2(x_1 y_2 - x_2 y_1)^2$, we have

$$\begin{aligned} & M^2((x_1 + \alpha y_1)^2 + (x_2 + \alpha y_2)^2) \\ &= M^2(x_1^2 + \alpha^2 y_1^2 + 2\alpha x_1 y_1 + x_2^2 + \alpha^2 y_2^2 + 2\alpha x_2 y_2) \\ &= 2\frac{M^2}{4}x_1^2 + M^2\alpha^2 y_1^2 + 2M^2\alpha x_1 y_1 + 2\frac{M^2}{4}x_2^2 + M^2\alpha^2 y_2^2 + 2M^2\alpha x_2 y_2 + 2\frac{M^2}{4}(x_1^2 + x_2^2) \\ &= M^2\alpha^2 y_1^2 + M^2\alpha^2 y_2^2 + 2M^2\alpha x_1 y_1 + 2M^2\alpha x_2 y_2 + 2x_2^2 y_1^2 + 2x_1^2 y_2^2 + 2\frac{M^2}{4}(x_1 - x_2)^2 \\ &\quad - 4x_1 x_2 y_1 y_2 + 2\left(\left(\frac{M^2}{4} - y_2^2\right)x_1^2 + \left(\frac{M^2}{4} - y_1^2\right)x_2^2\right) + 4x_1 x_2\left(\frac{M^2}{4} + y_1 y_2\right). \end{aligned} \quad (35)$$

Now we show the fact that the following phrase is always non-negative

$$\begin{aligned} A(M, \alpha) &= M^2\alpha^2 y_1^2 + M^2\alpha^2 y_2^2 + 2\alpha M^2 x_1 y_1 + 2\alpha M^2 x_2 y_2 + 2\left(\left(\frac{M^2}{4} - y_2^2\right)x_1^2 + \left(\frac{M^2}{4} - y_1^2\right)x_2^2\right) \\ &\quad + 2\frac{M^2}{4}(x_1 - x_2)^2 + 4x_1 x_2\left(\frac{M^2}{4} + y_1 y_2\right). \end{aligned} \quad (36)$$

By rewriting $A(M, \alpha)$ we have

$$A(M, \alpha) = M^2(y_1^2 + y_2^2)\alpha^2 + 2M^2(x_1 y_1 + x_2 y_2)\alpha + (M^2(x_1^2 + x_2^2) - 2(x_1 y_2 - x_2 y_1)^2). \quad (37)$$

After some algebraic operations, the discriminant of $A(M, \alpha)$ will be obtained as

$$\Delta_A = 4M^2(x_1 y_2 - x_2 y_1)^2(2(y_1^2 + y_2^2) - M^2) \leq 0, \quad (38)$$

where the last inequality results from the fact that $|y_1| \leq \frac{M}{2}$ and $|y_2| \leq \frac{M}{2}$. Because $\Delta_A \leq 0$ (and $M^2(y_1^2 + y_2^2) > 0$), for any value of α any combination of x_1, x_2, y_1 and y_2 , $A(M, \alpha)$ will be non-negative. Therefore, we continue (35) as

$$\begin{aligned} M^2((x_1 + \alpha y_1)^2 + (x_2 + \alpha y_2)^2) &= A(M, \alpha) + 2x_2^2 y_1^2 + 2x_1^2 y_2^2 - 4x_1 x_2 y_1 y_2 \\ &\geq 2x_2^2 y_1^2 + 2x_1^2 y_2^2 - 4x_1 x_2 y_1 y_2 = 2(x_1 y_2 - x_2 y_1)^2. \end{aligned} \quad (39)$$

So, $(x_1^*, y_1^*, x_2^*, y_2^*) = (-\frac{M}{2}, \frac{M}{2}, \frac{M(1-2\alpha)}{2}, \frac{M}{2})$ is the optimal choice to minimize $Q_\theta(x_1, y_1, x_2, y_2)$. However, $\frac{M(1-2\alpha)}{2}$ may not be an integer value. In order to decide whether higher or lower integer is the better choice, we simply check both of them in the function of $Q_\theta(x_1, y_1, x_2, y_2)$. The $Q_\theta(-\frac{M}{2}, \frac{M}{2}, x, \frac{M}{2})$ will be

$$Q_\theta(-\frac{M}{2}, \frac{M}{2}, x, \frac{M}{2}) = \frac{(1-\alpha)^2 + (\frac{2}{M}x + \alpha)^2}{(\frac{M}{2} + x)^2}.$$

As $\theta \rightarrow \frac{\pi}{4}$, $\frac{M(1-2\alpha)}{2} \rightarrow -\frac{M}{2}$, but because one antenna cannot be selected twice, the system will have to choose $1 - \frac{M}{2}$ for x_2 . The selection of $(-\frac{M}{2}, \frac{M}{2}, 1 - \frac{M}{2}, \frac{M}{2})$ happens when $\theta \geq \tan^{-1}(\frac{M-1}{M})$. Although this choice is optimal for a certain range of θ , after a point it will not be the best choice and $(x_1, y_1, x_2, y_2) = (-\frac{M}{2}, \frac{M}{2} - 1, 1 - \frac{M}{2}, \frac{M}{2})$ results in lower $Q_\theta(x_1, y_1, x_2, y_2)$. To obtain the range of θ that the latter set is the optimal choice, we have to solve the following inequality for α

$$Q_\theta(-\frac{M}{2}, \frac{M}{2} - 1, 1 - \frac{M}{2}, \frac{M}{2}) < Q_\theta(-\frac{M}{2}, \frac{M}{2}, 1 - \frac{M}{2}, \frac{M}{2}). \quad (40)$$

By replacing the actual values of both sides, we have

$$\frac{(\alpha - 1)^2(\frac{M^2}{2} - M + 1) + 2\alpha}{(M - 1)^2} < (\alpha - 1)^2 + \frac{(M(\alpha - 1) + 2)^2}{M^2}. \quad (41)$$

After some algebraic operations, (41) simplifies to

$$\begin{aligned} B(M, \alpha) &= M^2(3M^2 - 6M + 2)\alpha^2 - 2M(3M^3 - 10M^2 + 12M - 4)\alpha \\ &\quad + (M - 2)(3M - 2)(M^2 - 2M + 2) > 0. \end{aligned} \quad (42)$$

Calling α_{b_1} the smaller root and α_{b_2} the bigger root of $B(M, \alpha)$, for $M \geq 1 + \frac{1}{\sqrt{3}}$ ⁴ (which is the case because $M \geq 2$), the inequality of (42) is held when either $\alpha \leq \alpha_{b_1}$ or $\alpha_{b_2} \leq \alpha$. To find out which root indicates the value of θ_0 , after which $(x_1, y_1, x_2, y_2) = (-\frac{M}{2}, \frac{M}{2} - 1, 1 - \frac{M}{2}, \frac{M}{2})$ is the

⁴The roots of $(3M^2 - 6M + 2)$ are $1 \pm \frac{1}{\sqrt{3}}$ and for $M \geq 1 + \frac{1}{\sqrt{3}}$, the multiplier of α^2 will be always positive.

optimal choice, we investigate the sign of $B(M, \alpha)$ in a critical point in which $x_2 = \frac{M(1-2\alpha)}{2}$ is an integer and therefore $(x_1, y_1, x_2, y_2) = (-\frac{M}{2}, \frac{M}{2}, \frac{M(1-2\alpha)}{2}, \frac{M}{2})$ is still the optimal choice. This point is $\alpha = \frac{M-1}{M}$. By replacing $\alpha = \frac{M-1}{M}$ in $B(M, \alpha)$ and simplifying it, we obtain

$$B(M, \frac{M-1}{M}) = -M^2 - 2M + 2. \quad (43)$$

The roots of $B(M, \frac{M-1}{M})$ are $-\sqrt{3}-1$ and $\sqrt{3}-1$. So, for $M \geq 2$, (43) will always be negative (sign of M^2). This means that $\alpha = \frac{M-1}{M}$ is between the roots of $B(M, \alpha)$ (this is because for $M \geq 2$ the sign of $B(M, \alpha)$ is negative only between its root). We know that for $\alpha \leq \frac{M-1}{M}$, the optimal choice is $(x_1, y_1, x_2, y_2) = (-\frac{M}{2}, \frac{M}{2}, \frac{M(1-2\alpha)}{2}, \frac{M}{2})$ and therefore, the minimum α that changes the optimal choice, must be bigger than $\frac{M-1}{M}$. So, the minimum α after which the optimal choice becomes $(x_1, y_1, x_2, y_2) = (-\frac{M}{2}, \frac{M}{2} - 1, 1 - \frac{M}{2}, \frac{M}{2})$ is the bigger root of $B(M, \alpha)$ (solved for α). By noting that $\alpha = \tan(\theta)$, we obtain $\theta_0 = \tan^{-1}(\alpha_{b_2})$.

For $\theta_1 \leq \theta < \frac{\pi}{2}$, we relax the integer constraint only on y_2 to show that $(x_1, y_1, x_2, y_2) = (-\frac{M}{2}, \frac{M}{2}, -\frac{M}{2}, \frac{M(2-\alpha)}{2\alpha})$ is the optimal choice. By replacing $(x_1^*, y_1^*, x_2^*, y_2^*) = (-\frac{M}{2}, \frac{M}{2}, -\frac{M}{2}, \frac{M(2-\alpha)}{2\alpha})$ in (31) we have

$$f(x_1^*, y_1^*, x_2^*, y_2^*) = \frac{2\alpha}{M^2}. \quad (44)$$

The process to show that any other choice than $(x_1, y_1, x_2, y_2) = (-\frac{M}{2}, \frac{M}{2}, -\frac{M}{2}, \frac{M(2-\alpha)}{2\alpha})$ results in higher Q_θ is same as the process of (35). The only difference is that instead of showing $A(M, \alpha) \geq 0$, we should show that the following equation is non-negative:

$$C(M, \alpha) = (M^2(y_1^2 + y_2^2) - 2(x_1y_2 - x_2y_1)^2)\alpha^2 + 2M^2(x_1y_1 + x_2y_2)\alpha + M^2(x_1^2 + x_2^2). \quad (45)$$

The discriminant of $C(M, \alpha)$ will be obtained as

$$\Delta_C = 4M^2(x_1y_2 - x_2y_1)^2(2(x_1^2 + x_2^2) - M^2) \leq 0. \quad (46)$$

Same as (38), Δ_C in (46) is always non-positive, confirming that $C(M, \alpha) \geq 0$.

When θ is around $\frac{\pi}{4}$, $\frac{M(2-\alpha)}{2\alpha}$ is close to $\frac{M}{2}$ but as one antenna cannot be selected twice, system has to select $\frac{M}{2} - 1$ for y_2 . This obligation causes the choice of $(1 - \frac{M}{2}, \frac{M}{2}, -\frac{M}{2}, \frac{M}{2} - 1)$ to be the optimal choice for a certain range (same as the case of $\theta_0 < \theta < \frac{\pi}{4}$). To obtain this range, we have to solve the following inequality

$$Q_\theta(-\frac{M}{2}, \frac{M}{2} - 1, 1 - \frac{M}{2}, \frac{M}{2}) < Q_\theta(-\frac{M}{2}, \frac{M}{2}, -\frac{M}{2}, \frac{M}{2} - 1). \quad (47)$$

By replacing the actual values of both sides and simplifying the inequality we obtain

$$D(M, \alpha) = (M - 2)(3M - 2)(M^2 - 2M + 2)\alpha^2 - 2M(3M^3 - 10M^2 + 12M - 4)\alpha + M^2(3M^2 - 6M + 2) > 0. \quad (48)$$

Calling α_{d_1} the small root and α_{d_2} the big root of $D(M, \alpha)$, for $M > 2$ the inequality of (48) is held when either $\alpha \leq \alpha_{d_1}$ or $\alpha_{d_2} \leq \alpha$. To find out which root indicates the value of θ_1 , before which $(x_1, y_1, x_2, y_2) = (-\frac{M}{2}, \frac{M}{2} - 1, 1 - \frac{M}{2}, \frac{M}{2})$ is the optimal choice, we investigate the sign of $D(M, \alpha)$ in a critical point in which $y_2 = \frac{M(2-\alpha)}{2\alpha}$ is an integer and therefore $(x_1, y_1, x_2, y_2) = (-\frac{M}{2}, \frac{M}{2}, -\frac{M}{2}, \frac{M(2-\alpha)}{2\alpha})$ is still the optimal choice. This point is $\alpha = \frac{M}{M-1}$. By replacing $\alpha = \frac{M}{M-1}$ in $D(M, \alpha)$ and simplifying it, we obtain

$$D(M, \frac{M}{M-1}) = (-M^2 - 2M + 2)(\frac{M}{M-1})^2. \quad (49)$$

As $(\frac{M}{M-1})^2$ is always positive and the roots of $(-M^2 - 2M + 2)$ are $-1 \pm \sqrt{3}$, for $M > 1$, $D(M, \frac{M}{M-1}) < 0$. This means that $\alpha = \frac{M}{M-1}$ is between the roots of (48). We know that for $\alpha \geq \frac{M}{M-1}$, the optimal choice is $(x_1, y_1, x_2, y_2) = (-\frac{M}{2}, \frac{M}{2}, -\frac{M}{2}, \frac{M(2-\alpha)}{2\alpha})$ and therefore, the maximum α before which the optimal choice is $(x_1, y_1, x_2, y_2) = (-\frac{M}{2}, \frac{M}{2} - 1, 1 - \frac{M}{2}, \frac{M}{2})$ has to be the smaller root of (48). By noting that $\alpha = \tan(\theta)$, we obtain $\theta_1 = \tan^{-1}(\alpha_{d_1})$.

By comparing the (42) and (48) we see that both have same coefficient for α , and the α^2 coefficient in (42) is the constant term of (48) and vice versa. We know that the roots of $ax^2 + bx + c$ are $x_{1,2} = \frac{-b \pm \sqrt{b^2 - 4ac}}{2a}$ and the roots of $cx^2 + bx + a$ are $x_{3,4} = \frac{-b \pm \sqrt{b^2 - 4ac}}{2c} = \frac{a}{c}x_{1,2}$. Therefore, $\alpha_{d_1} = \frac{\alpha_{b_1} M^2 (3M^2 - 6M + 2)}{(M-2)(3M-2)(M^2 - 2M + 2)}$ and $\theta_1 = \tan^{-1}(\alpha_{d_1}) = \tan^{-1}(\frac{M^2 (3M^2 - 6M + 2) \alpha_{b_1}}{(M-2)(3M-2)(M^2 - 2M + 2)})$.